



# CHORUS

This is the accepted manuscript made available via CHORUS. The article has been published as:

## Single-Atom Heat Machines Enabled by Energy Quantization

David Gelbwaser-Klimovsky, Alexei Bylinskii, Dorian Gangloff, Rajibul Islam, Alán Aspuru-Guzik, and Vladan Vuletic

Phys. Rev. Lett. **120**, 170601 — Published 25 April 2018

DOI: [10.1103/PhysRevLett.120.170601](https://doi.org/10.1103/PhysRevLett.120.170601)

# Single-atom heat machines enabled by energy quantization

David Gelbwaser-Klimovsky\*,<sup>1</sup> Alexei Bylinskii,<sup>2</sup> Dorian Gangloff,<sup>3,4</sup>  
Rajibul Islam,<sup>5</sup> Alán Aspuru-Guzik,<sup>1</sup> and Vladan Vuletic<sup>4</sup>

<sup>1</sup>*Department of Chemistry and Chemical Biology, Harvard University, Cambridge, MA 02138\**

<sup>2</sup>*Department of Physics and Department of Chemistry and Chemical Biology, Harvard University, Cambridge, MA 02138*

<sup>3</sup>*Cavendish Laboratory, JJ Thomson Ave, Cambridge, UK, CB3 0HE*

<sup>4</sup>*Department of Physics and Research Laboratory of Electronics,  
Massachusetts Institute of Technology, Cambridge, MA 02139, USA*

<sup>5</sup>*Institute for Quantum Computing and Department of Physics and Astronomy,  
University of Waterloo, Waterloo, Ontario N2L 3G1, Canada*

Quantization of energy is a quintessential characteristic of quantum systems. Here we analyze its effects on the operation of Otto cycle heat machines and show that energy quantization alone may alter and increase machine performance in terms of output work, efficiency, and even operation mode. We show that this difference in performance occurs in machines with inhomogeneous energy level scaling, while quantum machines with homogeneous level scaling behave like classical machines. Our results demonstrate that quantum thermodynamics enables the realization of classically inconceivable Otto machines, such as those with an incompressible working substance. We propose to measure these effects experimentally using a laser-cooled trapped ion as a microscopic heat machine.

The discrepancy between classical and quantum mechanics, together with the fast progress on the control of open quantum systems such as ion traps [1–5], SQUIDS [6–8], quantum dots [9] and molecules [10], has ignited efforts to clarify the capabilities and thermodynamic limitations of quantum heat machines [11–14] under quantum effects such as coherences [15–17], quantum correlations [18, 19], quantum statistics of particles [20], squeezed thermal baths [21–23], many-body effects [24], and quantized work reservoirs [25–27]. Although these effects may offer classically inaccessible capabilities for machines, there has been no clear evidence that adiabatic quantum machines can outperform their classical counterparts once all non-equilibrium effects [28] and preparation costs are considered [29, 30]. Among the thermal machines, one of the most studied is the Otto machine [31, 32]. For this machine, most of the analyses have been limited to potential deformations that homogeneously scale all the energy levels. In this regime, a quantum and a classical heat machine have the same efficiency [32]. The few analyses that consider an inhomogeneous energy scaling [33, 34], have not show a clear advantage of a quantum heat machine over its classical counterpart.

In this Letter, we compare the performance of two *identical* heat machines based on trapped particles (working substance): one governed by classical mechanics and the other by quantum mechanics. We show that the discreteness of energy levels due to quantization, can increase the efficiency of a heat machine provided that the potential deformation creates an inhomogeneous shift of energy levels. We show that energy quantization can then: *i*) improve work extraction, cooling or efficiency

relative to the classical counterpart, even reaching the Carnot bound; *ii*) change the operation mode, e.g., a heat machine classically expected to operate as a refrigerator, may operate as an engine once energy quantization is considered; *iii*) enable operation at Carnot efficiency even in regimes where classically neither work extraction nor refrigeration are expected. The origin of the quantum enhanced performance can be traced to the change in relation between temperature and population distribution for adiabatic potential transformations with inhomogeneous energy level shifts. We emphasize that this analysis relies only on energy quantization and constant level populations in adiabatic potential transformations, and that it does not make use of any hidden resources like non-equilibrium or entangled baths [28].

Our results rely on the sensitivity of quantized energies to the boundaries, which classical systems are insensitive to. We illustrate this with an example of an Otto engine operated with an ideal gas contained in a one-dimensional (1D) infinite well potential (see Fig. 1A). The adiabatic introduction of a  $\delta$ -function barrier at the center does not alter the volume nor the classical energy, but by affecting the quantum wavefunctions, changes the energies of select quantum states. We show that this difference can result in superior performance of quantum heat engines.

Operated as a heat engine, an Otto machine (see Fig.1B and SI) transforms incoming heat from the hot bath,  $Q_h \geq 0$ , into extracted work,  $W < 0$ , with efficiency  $\eta^{en} = \frac{-W}{Q_h}$ . It consists of two adiabatic processes where the engine is decoupled from thermal baths, and two isochoric (constant volume) processes where the engine is coupled to two thermal baths at temperatures  $T_h$ ,  $T_c$ . Note that the efficiency of the Otto engine is not affected by the fact that the isochoric strokes are irreversible (see SI-VII and [36, 37]). Operated as a refrigerator it consumes work,  $W > 0$ , in order to cool down

---

\*Electronic address: dgelbwaser@fas.harvard.edu

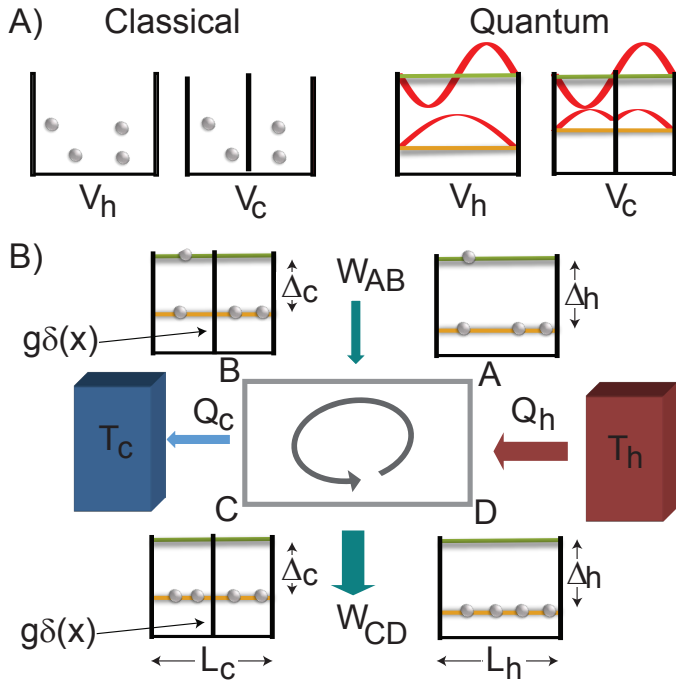


Figure 1: A) The adiabatic introduction of an infinite  $\delta$ -function barrier does not change the energy of a classical ideal gas (left), precluding classical work extraction, but shifts the energy of the quantum ground state (right) due to the non-zero amplitude of its wavefunction at the barrier position, enabling quantum work extraction. B) Quantum Otto cycle heat engine using the infinite well potential and the  $\delta$ -barrier. The cycle is composed of two adiabatic strokes (connecting states A and B, and C and D) where the potential is adiabatically deformed and the ion does not interact with any thermal bath, and two “isochoric” or “isoparametric” strokes [31] (connecting states B and C, and D and A) where the potential is kept constant while the ion equilibrates with the cold and the hot bath, respectively see the SI-VII. Work exchange results from the energy shift of the ground state while the excited state remains unshifted (for  $L_c = L_h$ ): work extraction  $W_{CD}$  takes place after thermalization with the cold bath and therefore at high ground-state population, whereas work injection  $W_{AB}$  takes place after thermalization with the hot bath and therefore at lower ground-state population. The difference between the ground-state populations results in net work extraction  $|W_{CD}| > |W_{AB}|$  at constant volume [35].

the cold bath by extracting heat from it,  $Q_c > 0$ , with efficiency  $\eta^{ref} = \frac{Q_c}{W}$ . We term heater the case where the heat flows in its “natural” direction from hot to cold,  $Q_h > 0$  and  $Q_c < 0$ , while no work is extracted,  $W \geq 0$ .

For a classical ideal gas in a uniform potential the compression ratio  $r = \frac{V_c}{V_h}$  defines the operation mode of the Otto cycle ( $V_{c(h)}$  is the container volume when the ideal gas is at equilibrium with the cold (hot) bath): i) for  $r \leq 1$  the machine is a heater; ii) for  $1 < r < r_{Car} \equiv \left(\frac{T_h}{T_c}\right)^{\frac{1}{\gamma-1}}$  it is an engine; iii) for  $r > r_{Car}$  it operates as a refrigerator. If run like an engine, the classical efficiency

is

$$\eta_{Otto}^{en} = 1 - \frac{1}{r^{\gamma-1}} \leq 1 - \frac{1}{r_{Car}^{\gamma-1}} \equiv \eta_{Car}^{en}, \quad (1)$$

where  $\gamma = \frac{C_p}{C_v}$  is the specific heat ratio and  $\eta_{Car}^{en}$  is the Carnot efficiency limit for an engine. For an incompressible gas,  $r = 1$  and  $\eta_{Otto}^{en} = 0$ . Classically, a compressible working substance is needed for work extraction, as it has been shown for classical rubber engines [38, 39] and classical continuum media [40, 41]. We show below that these paradigms break down once energy quantization is included in the analysis.

We first show that if the adiabatic potential deformation during the Otto cycle (from  $V_c$  to  $V_h$  and vice versa) is such that the energy levels scale as  $E_{n,h} = qE_{n,c}$ , where  $q$  is a positive constant independent of  $n$  (homogeneous scaling), then the classical and quantum heat machines always operate in the same mode with the same efficiency. Examples of this type of deformation are the frequency change of a 1D harmonic trap or the change of length of a 1D infinite square well potential. Under this assumption, the work (see SI-I) is

$$W = \frac{(1-q)}{q} \int_{qT_c}^{T_h} C_v dT, \quad (2)$$

where  $C_v \equiv \frac{\partial \langle H \rangle_T}{\partial T}$  is the heat capacity when the potential is  $V_h$ , and  $\langle \cdot \rangle_T$  is the expected value in the thermal Boltzmann distribution at temperature  $T$ . Similarly, the expressions for the heat transfers are:  $Q_h = \int_{qT_c}^{T_h} C_v dT$  and  $Q_c = -\frac{1}{q} \int_{qT_c}^{T_h} C_v dT$ . These expressions can also be derived from a completely classical treatment [42], where  $C_v$  is then the classical heat capacity. Efficiencies, being the ratio between work and heat, do not depend on the heat capacity for homogeneous energy scaling and under this condition are the same for classical and for quantum heat machines. However, the efficiency and even the operation mode can change when adiabatic potential deformations result in inhomogeneously scaled eigenenergies,  $E_{n,h} \neq qE_{n,c}$ .

To illustrate this, consider the Otto cycle shown in Fig. 1B where the potential is a 1D infinite well with variable length  $L$ , with a thin barrier of width  $\epsilon$  that can be adiabatically turned up to a height  $V_0$  at the center of the well. Here the energy of a classical particle in thermal equilibrium at temperature  $T$  is  $\langle H \rangle \approx \frac{1}{2}k_B T + V_0 \frac{\epsilon}{L} e^{-\frac{V_0}{k_B T}}$ . In the limit of an infinitesimally thin barrier  $\epsilon \rightarrow 0$  but constant  $g = V_0 \epsilon$ , the barrier becomes a  $\delta$ -function, the energy  $\langle H \rangle \rightarrow \frac{1}{2}k_B T$  becomes independent of the barrier, and the classical work output, cooling, and efficiency correspond to the classical Otto cycle with  $r = \frac{L_c}{L_h}$ , where  $L_{c(h)}$  is the well length at equilibrium with the cold (hot) bath.

By contrast, under quantum treatment, the even and odd eigenenergies are modified differently by introducing the delta barrier,  $g\delta(x)$  (see Fig. 1A) [43]. Odd

wavefunctions ( $\psi(x) = -\psi(-x)$ ) remain unperturbed,  $E_{n,c} = E_{n,h}$ , but  $E_{n,c} \neq E_{n,h}$  for even wavefunctions ( $\psi(x) = \psi(-x)$ ). In this case, the compression ratio remains  $r = 1$  and the classical efficiency is zero, while the quantum engine performs nearly at Carnot efficiency for a high repulsive barrier (see Fig. 2A). Measuring the work extraction during this potential deformation, or other transformation that do not change the “bulk” properties of the working substance, could be used to determine if the working substance is governed by classical or quantum laws.

Fig. 2B shows that, as one decreases the temperature of the baths at fixed temperature ratio,  $T_h/T_c$ , the system transitions from a classical regime, where many quantum states are populated, to a quantum regime with higher efficiency. In the limit of low temperature, where only the two lowest energy levels are appreciably populated, the work extraction condition and efficiency can be written as (see SI-II)

$$\frac{T_h}{T_c} \geq \frac{\Delta_h}{\Delta_c} > 1; \quad \eta = 1 - \frac{\Delta_c}{\Delta_h} = 1 - \frac{1}{r^2} \left( \frac{1}{1 - \frac{\Delta E_{c,\delta}}{\Delta_c}} \right), \quad (3)$$

where  $\Delta_h = E_{1,h} - E_{0,h}$  and  $\Delta_c = E_{1,c} - E_{0,c}$  are the energy gaps between excited and ground state when the system is in thermal contact with the hot and cold bath, respectively, and  $\Delta E_{c,\delta} \leq \Delta_c$  is the gap shift produced by the  $\delta$  barrier. Eq. 3 shows that the quantum Otto engine may extract work, at Carnot efficiency, for  $r = 1$  (fixed volume) or any other value of  $r$  (see dotted green line in Fig. 2A). Large  $g$  even enhances the efficiency at  $r < 1$ , effectively turning a classical heater into an engine. Negative  $g$  reduces the efficiency for  $r < r_{Car}$ , but turns a classically expected refrigerator into a highly efficient quantum engine for  $r > r_{Car}$ . Carnot efficient quantum engines for any compression ratio can be achieved beyond the two-level approximation. This requires extra control parameters, such as additional  $\delta$ -barriers, that will ensure that all the energy levels have the appropriate values. In the same way,  $g$  could be optimized for reaching maximum work extraction at any compression ratio or for producing maximum heat extraction,  $Q_c$ , or refrigeration efficiency  $\eta^{ref}$ .

The effects of quantization-induced work enhancement and operation mode change can be experimentally tested. To tune a given machine from classical to quantum, one can increase the potentials and temperatures by the same multiplicative factor,  $\xi^2$ . This effectively decreases the quantization scale relative to the bath temperature and as we show in SI-IV this scaling is equivalent to reducing  $\hbar$  to zero as  $\hbar_{eff} = \hbar/\xi$  (see Fig. 3C).

As a potential experimental platform we consider a trapped, laser-cooled ion in the combined electrostatic harmonic potential of a Paul ion trap and a sinusoidal potential of an optical lattice [2–4]. This potential can be used to mimic the infinite well with and without the

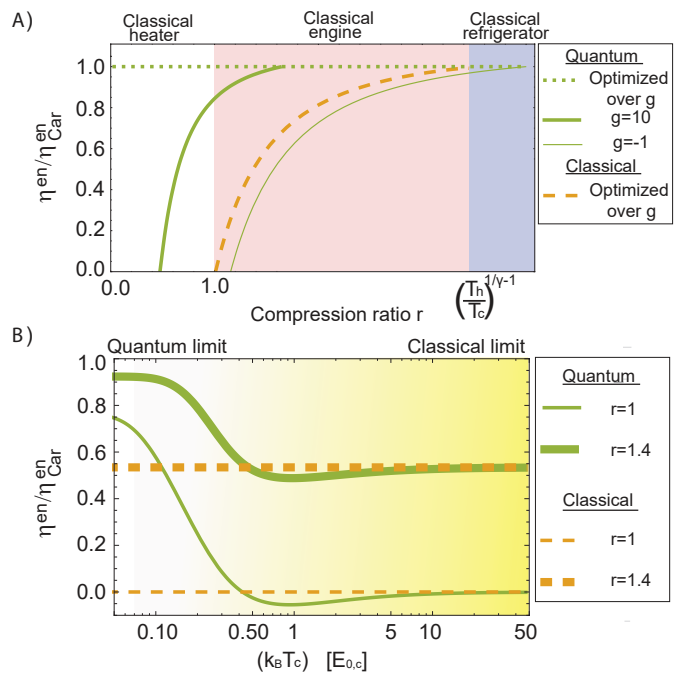


Figure 2: A) Efficiency normalized to Carnot efficiency for a classical (see SI-III) and quantum (see SI-I) Otto engine with a barrier of the form  $g\delta(x)$  (see Fig. 1B). The plane is divided into three areas depending on the classical operation mode (see Eq. (1) and the discussion below it). The temperature ratio is  $T_h/T_c = 12$ ,  $\gamma = 3$ ,  $g$  is given in units of the critical value  $g_{cri} = \frac{2\hbar^2}{mL_c}$ , and units are assumed such that  $\frac{2\hbar^2}{mL_h} = 1$ . B) Classical (dashed) and quantum (continuous) normalized efficiency as function of  $T_c$ , for  $r = 1.4$  (thick) and  $r = 1$  (thin), and fixed ratio  $T_h/T_c$  for an ideal gas. The temperature dependence is a signature of the quantum machine. The number of populated levels depends on the temperature.

$\delta$ -barrier. The potential has the form

$$V_i(x) = m\omega_i^2 a^2 \left( \frac{1}{2} (x/a)^2 + \frac{\kappa_i}{4\pi^2} (1 + \cos(2\pi x/a)) \right), \quad (4)$$

where  $\kappa_i = \omega_{L,i}^2/\omega_i^2$  is the dimensionless parameter controlling the shape of the potential (see Fig. 3A), given by the squared ratio of lattice vibrational frequency  $\omega_{L,i} = \sqrt{\frac{2\pi^2 U_i}{ma^2}}$  to the harmonic trap vibrational frequency  $\omega_i$ . Here  $U_i$  is the depth of the lattice potential. For  $\kappa_i = 1$ , the potential is a single well while for  $\kappa_i > 1$ , the potential is a double-well, or, equivalently, a single well with a barrier in the middle. The parameter  $\kappa_i$  can be tuned by tuning  $U_i$  (via laser power) and/or the vibrational frequency of the harmonic potential  $\omega_i$  (by applying voltage to the Paul trap electrodes). In Fig. 3B we show computational results based on discrete variable representation (DVR) calculations [44] for the work extraction and efficiency of the classical and quantum versions of the Otto cycle shown in Fig. 1B, but implemented with the ion-trap potential (Eq. (4)) by adiabatically tuning  $\kappa_i$  and  $\omega_i$  in order to generate a double-well and flat-bottom poten-

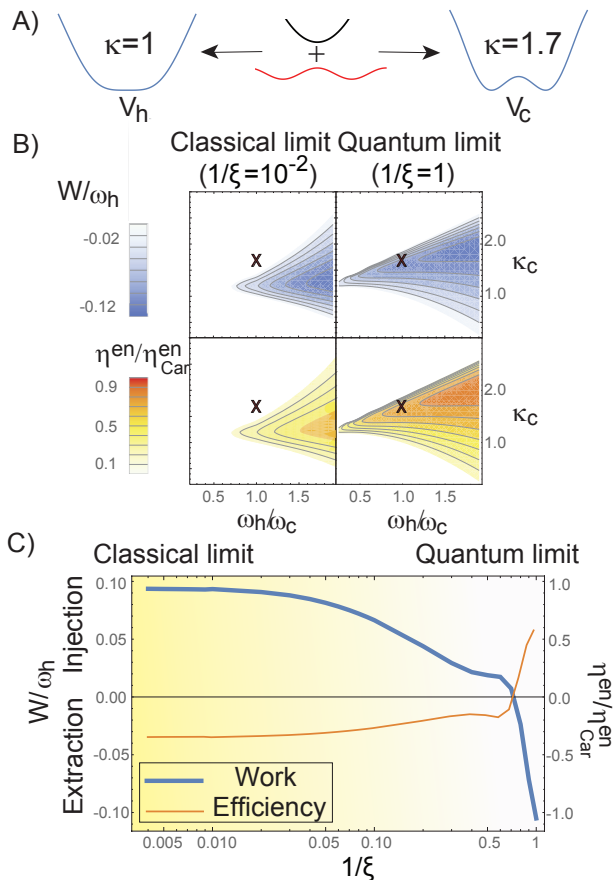


Figure 3: A) The proposed experimental potential (see Eq. (4)). B) Calculated work (top) and normalized efficiency (bottom) for the classical (left) and quantum limit (right). Here  $\kappa_h = 1$  and  $\omega_h = 1$  MHz have been chosen. The white areas correspond to the heater. The “X” indicates the parameters used for Fig. 3C,  $\kappa_c = 1.7$  and  $\omega_c = \omega_h$ , where the classical heater operates as a heat engine in the quantum limit. C) Calculated work and efficiency. The classical limit is obtained at  $\frac{1}{\xi} \rightarrow 0$ , where the work becomes constant and positive (work injection). In contrast, at the quantum limit,  $\frac{1}{\xi} = 1$ , work is extracted. Cycle parameters:  $T_h/T_c = 41.6$ ,  $\bar{n}_c = 0.033$ .

tial. As shown by the marked “X”, there are parameters for which a classical heater operates as a quantum engine once energy quantization is considered. Fig. 3C shows the DVR results as function of  $\frac{1}{\xi}$  for the parameters of the point “X” on Fig. 3B. The sign of work flips from positive (work injection) to negative (work extraction) when going from the classical to the quantum limit. Thus, the turning of a heater into an engine by energy quantization is directly observable in a realistic experimental setup.

During the isochoric strokes the ion is continuously laser-cooled; at steady-state its temperature is fixed at a stable point where the laser cooling rate balances the heating rate by the environment. The occupation of energy levels then approximately follows a thermal distribution and the system can be considered to be in contact with a thermal bath [45, 46]. Contact to a cold ther-

mal bath is achieved by optimizing laser cooling parameters to reduce the steady-state temperature of the ion, whereas contact to a hot thermal bath is achieved by choosing sub-optimal cooling parameters. Raman sideband cooling of  $^{174}\text{Yb}^+$  in an  $\omega_{L,i} \sim 2\pi \times 10$  MHz lattice has been shown to reach near ground-state occupation  $\bar{n} \sim 0.1$ , and the temperature has been increased controllably by up to a factor of 10 [2–4]. This range could be further increased by reducing external heating sources, and using a narrow optical transition to precisely measure the motional quantum state populations and ion temperature [47]. The total energy stored in the system  $E_T = \sum_n p_n E_n$  at different times can thus be measured via resolved vibrational mode spectroscopy to determine the energy eigenspectrum  $E_n$ , and populations  $p_n$  [45]. From these measurements, the total work output per cycle can be obtained, and the experiment can be performed in the quantum and classical limits to identify the effects of quantization.

For the adiabatic strokes the laser cooling is disconnected. Perfect adiabaticity has been assumed in the calculation above. In practice, potential deformations during the Otto cycle have to be performed at finite speed, and to avoid excitations that perturb the population distribution, the total adiabatic ramp time must be longer than the inverse of the smallest energy spacing. Yet, the ramp time must be shorter than the thermalization time set by the background heating in the range  $\sim 1 - 1000$  motional quanta per second [48]. These two conditions can be fulfilled simultaneously for trap vibration frequencies in the MHz range.

We have shown that a quantum Otto engine can be more efficient than its classical counterpart, but that both are subject to the Carnot limit. This performance difference may be significant since the efficiency of real heat engines [49] is limited by the practical difficulty to reach large compression ratios. Moreover, we have shown that classically well established paradigms no longer hold in the quantum regime, where energy quantization allows engines to operate at Carnot efficiency even for compression ratios  $r < 1$ ,  $r > \left(\frac{T_h}{T_c}\right)^{\frac{1}{\gamma-1}}$  and  $r = 1$  (fixed volume), which could enable the realization of Otto engines with incompressible working substances. These results still hold for a simple model of finite time or imperfect thermalization during the isochoric strokes (see SI-VI), but more detailed studies are needed to clarify the difference between quantum and classical finite time heat machines.

Since a heat machine operating at given bath temperatures is only characterized by two parameters, the efficiency  $\eta$  and the work  $W$ , it is always possible to construct a classical machine that mimics a quantum machine with the same  $\eta$  and  $W$ , by choosing a different compression ratio, working fluid, potential deformation, etc. However, here we are interested in differentiating performance changes based on the quantum/classical nature of the working substance from those originating from other parameter differences. As we have shown, energy

quantization, of purely quantum origin, can give rise to a marked difference in performance.

Energy quantization depends on boundary effects, that generally can be neglected for classical thermodynamic systems, but at the quantum regime allow for work extraction without changing any bulk property of the working substance such as length for a 1D system (or volume for 3D).

Finally, we have shown that for the studied system non-classical results can be only found when energy levels are inhomogeneously scaled. This regime has rarely been analyzed and requires further investigation. Some potential future research paths include the performance of other thermodynamic cycles (i.e., Carnot, Stirling, etc),

or the use of a working substance composed of interacting particles or indistinguishable particles (Fermions and Bosons).

### Acknowledgments

D. G.-K. and A. A.-G. acknowledge the support from the Center for Excitonics, an Energy Frontier Research Center funded by the U.S. Department of Energy under award DE-SC0001088 (Energy conversion). V.V. acknowledges support from the NSF (PHY-1505862) and the NSF CUA (PHY-1125846).

- 
- [1] J. Roßnagel, O. Abah, F. Schmidt-Kaler, K. Singer, and E. Lutz, *Science* **352**, 325 (2016).
  - [2] L. Karpa, A. Bylinskii, D. Gangloff, M. Cetina, and V. Vuletić, *Phys Rev Lett* **111**, 163002 (2013).
  - [3] A. Bylinskii, D. Gangloff, and V. Vuletić, *Science* **348**, 1115 (2015).
  - [4] D. Gangloff, A. Bylinskii, I. Counts, W. Jhe, and V. Vuletić, *Nature Phys* **11**, 915 (2015).
  - [5] D. Leibfried, R. Blatt, C. Monroe, and D. Wineland, *Rev Mod Phys* **75**, 281 (2003).
  - [6] A. Fornieri, C. Blanc, R. Bosisio, S. D'Ambrosio, and F. Giazotto, *Nature Nanotechnol* (2015).
  - [7] A. Bylinskii, D. Gangloff, I. Counts, and V. Vuletić, *Nat Mater* **15**, 717 (2016).
  - [8] A. Bylinskii, Ph.D. Thesis, MIT (2015).
  - [9] B. Sothmann, R. Sánchez, and A. N. Jordan, *Nanotech* **26**, 032001 (2014).
  - [10] C. Lotze, M. Corso, K. J. Franke, F. von Oppen, and J. I. Pascual, *Science* **338**, 779 (2012).
  - [11] D. Gelbwaser-Klimovsky, W. Niedenzu, and G. Kurizki, *Adv AMOP* **64**, 329 (2015).
  - [12] R. Kosloff, *Entropy* **15**, 2100 (2013).
  - [13] G. Xiao and J. Gong, *Physical Review E* **92**, 012118 (2015).
  - [14] A. Roulet, S. Nimmrichter, J. M. Arrazola, S. Seah, and V. Scarani, *Physical Review E* **95**, 062131 (2017).
  - [15] R. Uzdin, A. Levy, and R. Kosloff, *Phys Rev X* **5**, 031044 (2015).
  - [16] M. O. Scully, K. R. Chapin, K. E. Dorfman, M. B. Kim, and A. Svidzinsky, *PNAS* **108**, 15097 (2011).
  - [17] D. Gelbwaser-Klimovsky, W. Niedenzu, P. Brumer, and G. Kurizki, *Sci Rep* **5** (2015).
  - [18] L. A. Correa, J. P. Palao, G. Adesso, and D. Alonso, *Phys Rev E* **87**, 042131 (2013).
  - [19] M. Perarnau-Llobet, K. V. Hovhannisyanyan, M. Huber, P. Skrzypczyk, N. Brunner, and A. Acín, *Phys Rev X* **5**, 041011 (2015).
  - [20] Y. Zheng and D. Poletti, *Phys Rev E* **92**, 012110 (2015).
  - [21] J. Roßnagel, O. Abah, F. Schmidt-Kaler, K. Singer, and E. Lutz, *Phys Rev Lett* **112**, 030602 (2014).
  - [22] W. Niedenzu, D. Gelbwaser-Klimovsky, A. G. Kofman, and G. Kurizki, *New J Phys* **18**, 083012 (2016).
  - [23] G. Manzano, F. Galve, R. Zambrini, and J. M. Parrondo, *Phys Rev E* **93**, 052120 (2016).
  - [24] J. Jaramillo, M. Beau, and A. del Campo, *New J Phys* **18**, 075019 (2016).
  - [25] A. Levy, L. Diósi, and R. Kosloff, *Phys Rev A* **93**, 052119 (2016).
  - [26] N. Linden, S. Popescu, and P. Skrzypczyk, *Phys Rev Lett* **105**, 130401 (2010).
  - [27] D. Gelbwaser-Klimovsky and G. Kurizki, *Phys Rev E* **90**, 022102 (2014).
  - [28] R. Alicki and D. Gelbwaser-Klimovsky, *New J Phys* **17**, 115012 (2015).
  - [29] Y. Zheng, S. Campbell, G. De Chiara, and D. Poletti, *Physical Review A* **94**, 042132 (2016).
  - [30] E. Torrontegui, I. Lizuain, S. González-Resines, A. Tobalina, A. Ruschhaupt, R. Kosloff, and J. G. Muga, *Physical Review A* **96**, 022133 (2017).
  - [31] Y. Zheng and D. Poletti, *Phys Rev E* **90**, 012145 (2014).
  - [32] H. Quan, Y.-x. Liu, C. Sun, and F. Nori, *Phys Rev E* **76**, 031105 (2007).
  - [33] R. Uzdin and R. Kosloff, *New Journal of Physics* **16**, 095003 (2014).
  - [34] H. Quan, P. Zhang, and C. Sun, *Physical Review E* **72**, 056110 (2005).
  - [35] N. Sandoval-Figueroa and V. Romero-Rochín, *Phys Rev E* **78**, 061129 (2008).
  - [36] H. S. Leff and G. L. Jones, *American Journal of Physics* **43**, 973 (1975).
  - [37] D. Mukhopadhyay and K. Bhattacharyya, arXiv preprint arXiv:0911.5010 (2009).
  - [38] R. J. Farris, *Rubber Chemistry and Technology* **52**, 159 (1979).
  - [39] J. Mullen, G. W. Look, and J. Konkel, *Am. J. Phys* **43**, 349 (1975).
  - [40] S. Paolucci, *Continuum mechanics and thermodynamics of matter* (Cambridge University Press, 2016).
  - [41] M. E. Gurtin, E. Fried, and L. Anand, *The mechanics and thermodynamics of continua* (Cambridge University Press, 2010).
  - [42] W. Greiner, L. Neise, and H. Stöcker, *Thermodynamics and statistical mechanics* (Springer Science & Business Media, 2012).
  - [43] M. Belloni and R. W. Robinett, *Physics Reports* **540**, 25 (2014).
  - [44] D. T. Colbert and W. H. Miller, *J Chem Phys* **96**, 1982 (1992).

- [45] S. An, J.-N. Zhang, M. Um, D. Lv, Y. Lu, J. Zhang, Z.-Q. Yin, H.-T. Quan, and K. Kim, *Nature Phys* **11**, 193 (2015).
- [46] D. Meekhof, C. Monroe, B. King, W. Itano, and D. Wineland, *Phys Rev Lett* **76**, 1796 (1996).
- [47] K. Johnson, B. Neyenhuis, J. Mizrahi, J. Wong-Campos, and C. Monroe, *Phys Rev Lett* **115**, 213001 (2015).
- [48] A. M. Eltony, D. Gangloff, M. Shi, A. Bylinskii, V. Vuletić, and I. L. Chuang, *Quantum Information Processing* **15**, 5351 (2016).
- [49] F. Curzon and B. Ahlborn, *American Journal of Physics* **43**, 22 (1975).